Copper Substrate Catalyzes Tetraazaperopyrene Polymerization

W.G. Schmidt, E. Rauls, U. Gerstmann, S. Sanna, M. Landmann, M. Rohrmüller, A. Riefer, S. Wippermann, and S. Blankenburg

Abstract The polymerization of tetraazaperopyrene (TAPP) molecules on a Cu(111) substrate, as observed in recent STM experiments, has been investigated in detail by first principles calculations. Tautomerization is the first step required for the formation of molecular dimers and polymers. The substrate is found to catalyze this tautomerization.

1 Introduction

The ongoing miniaturization of electronic devices drives the search for alternatives to the present approaches of lithographic manufacturing. In this context, the spontaneous ordering and assembly of atoms and molecules on atomically well-defined surfaces, the so-called bottom-up approach, appears to be a very promising way to fabricate functional systems with nanometer dimensions [1–3].

The intermolecular interactions ranging from indirect, substrate mediated interplay [4] and direct Coulomb forces [5] to weak dispersion interactions, metal complexation [6] and hydrogen [7, 8] or covalent bonds [9] set the stage for a large number of possibilities to form one- and two-dimensional molecular networks of varying robustness. Many potential applications of supramolecular structures, e.g., as templates in bottom-up device technology will require a thermal and chemical stability that can only be achieved by covalent bonding. Layers in which the adsorbates are interlinked by strong covalent bonds are advantageous also in the field of organic

---

W.G. Schmidt · E. Rauls · U. Gerstmann · S. Sanna · M. Landmann · M. Rohrmüller · A. Riefer
Lehrstuhl für Theoretische Physik, Universität Paderborn, 33095 Paderborn, Germany

S. Wippermann
University of California, Dept. of Chemistry, One Shields Avenue, Davis, CA 95616, USA

S. Blankenburg
Eidgenössische Materialprüfungs- und Forschungsanstalt (EMPA), 8600 Dübendorf, Switzerland

W.E. Nagel et al. (eds.), *High Performance Computing in Science and Engineering '11*, DOI 10.1007/978-3-642-23869-7_4,

electronics, e.g., for organic field effect transistors or organic solar cells. Provided nanoporous molecular networks are sufficiently robust, they may also offer well-defined surroundings to control surface chemical reactions in confined spaces. For these reasons a number of experimental investigations into covalently interlinked molecular structures on surfaces under ultrahigh vacuum (UHV) conditions were performed. For instance, the vapor-deposition polymerization of ultrathin films was studied by scanning tunneling microscopy (STM) [10, 11]. The STM was not only used to study, but also to initialize and control the polymerization of adsorbates [12]. Photoinduced polymerization of surface adsorbed diacetylene was demonstrated to allow for the switching between different adsorbate phases [13]. Recent years have seen a surge of interest in the formation and characterization of two-dimensional, covalent organic networks based on chemical reactions at surfaces, see, e.g., Refs. [8, 14–23].

Using computer grants of the HLRS, we studied the tautomerization reaction of 1,3,8,10-tetraazaperopyrene (TAPP) on a Cu(111) surface on the basis of DFT calculations [24]. This special system has previously been investigated experimentally by Matena et al. [16, 23]. The authors found that the copper substrate is crucial for the formation of the various aggregates they observed, i.e. differently ordered close-packed as well as porous networks on the one hand, and covalently bonded linear chains on the other hand. From a surface science point of view, especially the latter are of great interest, since their formation requires a multiple step chemical reaction which does not occur in gas phase. The Cu(111) surface exhibits only a weak interaction with the adsorbed molecules, but obviously is sufficient to change the reaction kinetics. Recent DFT calculations focused on the energetic stability of the molecular network or the chain, respectively [23, 25]. However, the detailed mechanism for the tautomerization reaction has not been investigated yet. With the work presented here, we want to close this gap.

2 Computational Method

The DFT calculations are performed within the local density approximation (LDA) for exchange and correlation as implemented in VASP [26]. Thereby the system of Kohn-Sham equations

$$\left\{-\frac{\hbar^2}{2m}\triangle + V_{ext}(\boldsymbol{r}) + \int \frac{n(\boldsymbol{r}')}{|\boldsymbol{r}-\boldsymbol{r}'|}d\boldsymbol{r}' + V_{xc}(\boldsymbol{r})\right\}\psi_{n\boldsymbol{k}}(\boldsymbol{r}) = \varepsilon_{n\boldsymbol{k}}\psi_{n\boldsymbol{k}} \tag{1}$$

$$n(\boldsymbol{r}) = \sum_{n,\boldsymbol{k}} f_{n\boldsymbol{k}}|\psi_{n\boldsymbol{k}}|^2 \tag{2}$$

is solved iteratively for the external potential $V_{ext}(\boldsymbol{r})$ until self-consistency in the total electron density $n(\boldsymbol{r})$ is reached. Plane waves serve as basis set for the Kohn-Sham orbitals $\psi_{n\boldsymbol{k}}(\boldsymbol{r})$. The ground-state DFT calculations were parallelized for different bands and sampling points in the Brillouin zone using the message passing

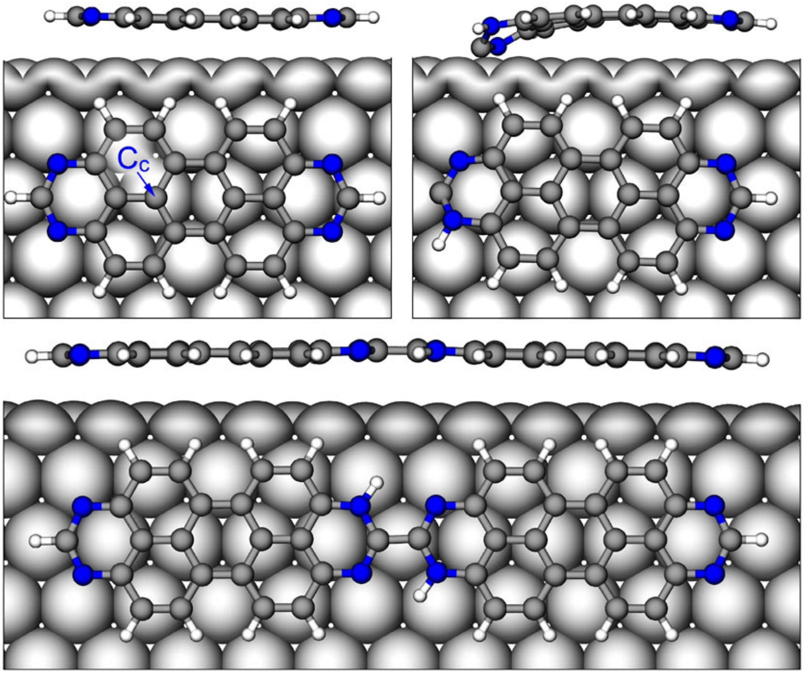

Fig. 1 Molecular model for the single TAPP molecule (left), the first tautomer TA1 (right) and the dimer adsorbed on the Cu(111) surface (bottom)

interface (MPI). Parallelization over bands and plane wave coefficients at the same time reduces the communication overhead significantly.

In order to account approximately for the influence of the dispersion interaction, a semiempirical scheme based on the London dispersion formula was used [27, 28]. The electron-ion interaction was described by the projector-augmented wave (PAW) method [29, 30], which allows for an accurate treatment of the first-row elements as well as the Cu $3d$ electrons with a relatively moderate energy cutoff of 340 eV. The adstructures were modeled in periodically repeated supercells, containing two atomic Cu layers arranged in a $\left(\begin{smallmatrix}14 & 0\\ 3 & 6\end{smallmatrix}\right)$ translational symmetry, the adsorbed molecules and a vacuum region of 15 Å. Adsorption energies were obtained as $E_{ads} = E_{tot} - E_{sub} - E_{mol} - N_{Cu}\mu_{Cu} + \frac{1}{2}N_H E_{H_2}$ from the total energy of the adsystem E_{tot}, the substrate E_{sub} and the molecule E_{mol}. Here the number of additional metallic adatoms is given by N_{Cu}, N_H denotes the number of dissociated hydrogens, μ_{Cu} is the copper adatom chemical potential and E_{H_2} the energy of molecular hydrogen. Potential energy surfaces (PES) are calculated by lateral displacement of the molecule followed by a relaxation with a laterally constrained carbon atom (C_c in Fig. 1).

Figure 2 shows benchmark calculations to determine the electronic ground state of a typical 150 atom cell used for surface modeling in our project. The calculations within this project were performed on the NEC SX-8 and SX-9 of the

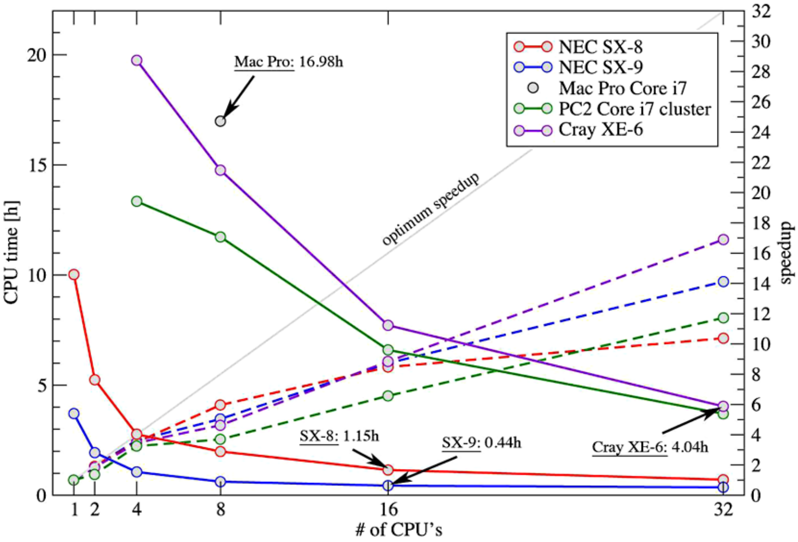

Fig. 2 CPU time and speedup for DFT calculations for Perfluoro-anthracene (PFA) on the Au(111) surface containing around 150 atoms. The calculations were performed with the Stuttgart optimized VASP version on the HLRS NEC SX-8 and SX-9 machines. In comparison, we show data for the HLRS Cray XE6, a local Linux cluster (Intel Core i7, 24 Twin-nodes with 4 CPUs 2.5 GHz Quad Core Xeon each) and Mac Pro workstations (Intel Core i7)

Höchstleistungsrechenzentrum Stuttgart. As can be seen, a reasonable scaling is achieved for using up to 32 CPUs.

3 Results

A single TAPP molecule adsorbs completely flat on the Cu(111) surface. The adsorption geometry can be seen in the top left part of Fig. 1. The molecule–substrate interaction is weak and dominated by dispersion forces. The molecule's center ring is located on top of a copper atom as energetically most favorable adsorption position. In this minimum energy position, the adsorption energy amounts to −2.55 eV. However, due to the weak interaction with the substrate and its mainly dispersive character, the molecule can be expected to be rather mobile, which is crucial for the polymerization reactions discussed in the following. The calculated PES (Fig. 2 in Ref. [24]) indicates only small energy barriers hindering lateral movements of the molecule at the surface. The movement of the center ring of the molecule to a bridge site increases the energy by less than 0.01 eV, and even the most unfavorable hollow site is only by 0.02 eV less favorable in energy than the top site.

Tautomerization is an essential prerequisite for chain and network formation of the TAPP molecules. The hydrogen atom at the central edge carbon has to move to one of the adjacent nitrogen atoms in order to form the first tautomer (TA1, cf.

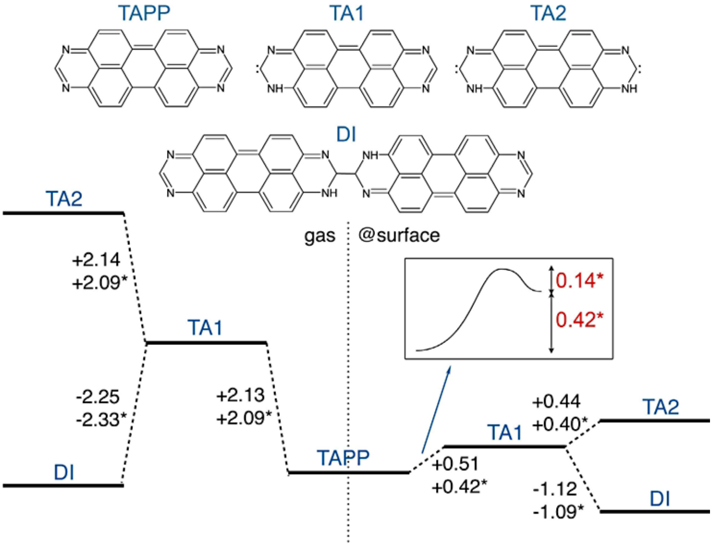

Fig. 3 Energetics of the reaction. Towards the left, results for the gas phase are shown. Towards the right, the reaction on the substrate is shown. All values in eV/molecule. Energies including dispersion corrections are marked with an asterisk. See text for details

Fig. 1). In this configuration, the central carbon is left with only two bonds to the neighboring nitrogen atoms and a free electron pair. The same reaction happens for the second tautomer (TA2) at the central edge carbon at the opposite side of the molecule. With an energy difference of 2.09 eV between TAPP and TA1, the described tautomerization process is unfavorable in gas phase (see Fig. 3 for an overview of the energetics). Analogously, the same holds for the formation of TA2. In gas phase, the polymerization is hindered due to this costly removal of the hydrogen atom.

The energetics change significantly for Cu(111) adsorbed molecules. However, the polymerization process is preceded by a copper coordination network, and additional surface adatoms may also modify the reaction kinetics. To get an idea of the impact of the various processes, we start with the discussion of the clean unperturbed surface followed by the discussion of the copper adatom influence.

Since the TA1 tautomer can deform after desorption and bind covalently to a Cu atom, the adsorbate system can remain in an energetically more favorable geometry than in the gas phase. Thus, the energetic difference between TAPP and TA1 (in the adsorbed geometry) decreases by a factor of five to 0.42 eV. Figure 1 shows the adsorption geometries for TAPP (top left part of the figure) and TA1 (top right part).

The diffusion barrier of the tautomer TA1 (TA2) is higher than that of TAPP and amounts to 0.5 eV (0.7 eV). Also the energetically favored bonding position for both tautomers is shifted towards the bridge side with respect to the central ring of the molecule. Therefore, the mobility of the tautomers is reduced compared to the TAPP molecule suggesting covalent bonding to the substrate. This is supported by

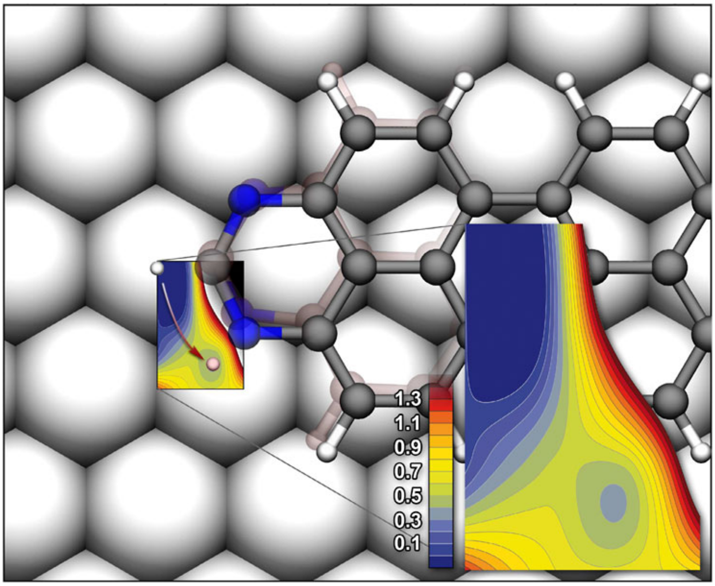

Fig. 4 PES (including dispersion corrections) of the tautomerization process from TAPP towards TA1 (one hydrogen moves from the carbon to the nitrogen). All values in eV

the calculated charge density differences revealing that the free electron pair of the central carbon atom of the TA1 tautomer binds to the substrate. Additionally, the nitrogen lone pair interacts weakly with the surface. At this point, the catalyzing effect of the surface can to some extent already be understood.

While the total energy differences between the tautomers explain the relative stabilities, the activation energies for the tautomerization reactions have to be calculated in order to understand the reaction kinetics.

We have calculated the PES for the moving hydrogen both for the molecule in the gas phase and in the adsorbed state (Fig. 4). The barrier for the first tautomerization (TAPP → TA1) is found to be significantly smaller in the adsorbed state (0.56 eV) than in the gas phase (2.10 eV). Figure 4 shows the path taken by the H-atom during the tautomerization process in the adsorbate state and reveals that the final state is a local energy minimum. An energy barrier of 0.14 eV separates this state from the initial configuration (TAPP). In the gas phase, in contrast, TA1 is not stable, since the energy barrier for the reverse reaction (TA1 → TAPP) is with 0.01 eV negligible and even within the error bar of our calculations. Thus, on the substrate, TA1 can be viewed as a meta stable state. This fact, together with the total energy differences discussed above, enhances the tautomerization and makes the reaction, contrary to the gas phase, likely to happen at the substrate.

The tautomerization is the first step towards chain or network formation. The second step towards the formation of longer polymers is the dimerization of two tautomers. The formation of a dimer (DI) consisting of two TA1 tautomers is highly favored at the substrate as well as in the gas phase. The energy gain has been calculated to be by a factor of two higher in gas phase (-2.33 eV) than at the substrate (-1.09 eV). One reason for this is that the isolated TA1 tautomer is unstable in gas phase, another reason is the covalent bonding of TA1 to the substrate which has to be lifted for the dimer bond formation. Since the dimer has a flat adsorption geometry (see bottom part of Fig. 1), the molecule-substrate bonds of TA1 must be broken. Nevertheless, there is an overall energy gain due to the formation of a C=C double bond between the two TA1. Comparing DI with the originating TAPP, this energy gain is by a factor of two higher for the molecules adsorbed on the Cu-surface than in gas phase. Figure 3 summarizes the results of our calculations in a reaction diagram. Starting from the TAPP molecule in the center, the two step process via TA1 to DI is shown for the gas phase (towards the left) or for the adsorbate (towards the right), respectively. Values marked with an asterisk include dispersion interactions, while those without are DFT-GGA values. Although the dispersive interaction is the main contribution to the binding energy of TAPP to the substrate, it does not change the reactions qualitatively, as could have been expected based on our previous experiences with comparable systems [31]. An explanation for this finding might be the crucial role of the formation of covalent bonds for TA1. From TA1, the second tautomerization step to TA2 is in both cases unlikely. For chain formation, however, it is not needed. The deformation of the adsorbed TA1 due to the bond to the substrate does not affect more than half of the molecule. The other end of the molecule remains approximately flat. In DI, the situation is similar, thus deformation is not hindered and the mechanism of the repositioning of the hydrogen atom at the DI central C can happen completely analogously to the reaction from TAPP to TA1. Like this, a third and any further TA1 can be added, resulting in linear molecular chains.

However, additional adatoms can also play a crucial role during the covalent synthesis. Figure 5 summarizes the potential influence of Cu adatoms on the reaction process. Hereby, the energy levels depend on the chemical potential of the adatoms μ_{Cu}. It ranges from the energy of copper bulk μ_{Cu}^{bulk} up to the adsorption energy of a single isolated adatom μ_{Cu}^{adatom}. This range is shown in Fig. 5 with shaded areas. We first discuss the case that the system is in equilibrium with a copper bulk reservoir, i.e., adatoms are not freely available but have to generated from the substrate bulk.

For the single TAPP one molecular nitrogen is coordinated to the metal and the energy difference of 0.09 eV compared to the clean surface shows a slight preference of the non-coordinated geometry for lower coverages. After the first tautomerization, the total-energy difference between coordinated and non-coordinated TA1 increases to 0.38 eV. Now, the central carbon is bonded to the additional metal atom resulting just in a small deviation from the planar structure which reduces the strain of the molecule compared to the uncoordinated case. The corrugation of the PES decreases for the TA1-M tautomer compared to the uncoordinated case from 0.6 eV to 0.15 eV as seen in Fig. 2 in Ref. [24]. Thus, the metal coordination reduces the diffusion hinderance of the tautomer.

The hydrogen diffusion from the molecule to the substrate possibly assisted by the metal adatom is another possibility to form the TA1 state. The resulting molecule is now partially dehydrogenated and bonds to the coordination atom. However, this

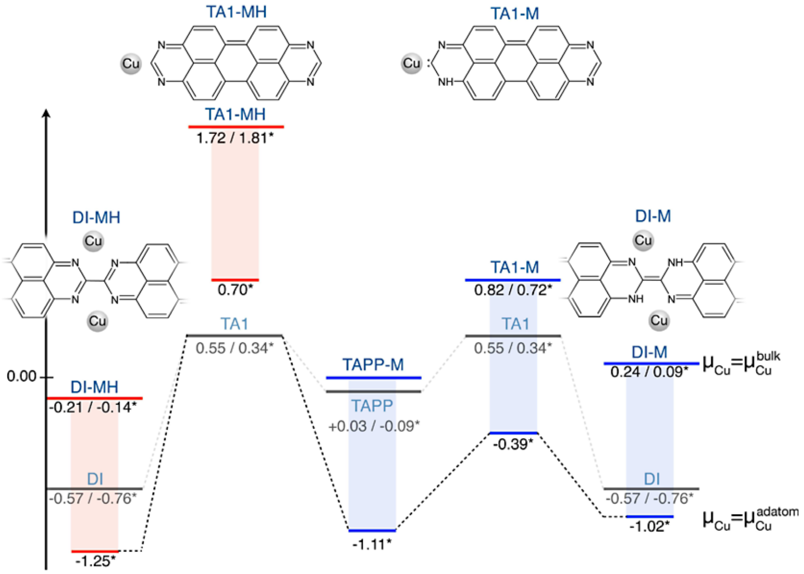

Fig. 5 Energetics of the reaction with coordination adatoms (right) and an additional dehydrogenation (left). The corresponding molecular structures are visualized as well. The ranges of the chemical potentials of copper are marked with shaded areas for metal coordinated structures (ranging from μ_{Cu}^{bulk} to μ_{Cu}^{adatom} as indicated). All values in eV/molecule. Energies including dispersion corrections are marked with an asterisk. See text for details

increases the energy by 1.81 eV and is thus not likely. The dimerization of two TA1 tautomers results in an energy gain for all three possibilities: DI with metal coordination (-0.25 eV), DI with metal coordination and hydrogen loss (-0.48 eV) as well as DI (-1.09 eV). The dehydrogenated state DI-MH is now more stable than the solely coordinated dimer (DI-M). Nevertheless, for the upper limit of the chemical potential, the uncoordinated reaction pathway as described above is preferred.

Indeed, at high temperatures there are additional adatoms available due to thermal degradation from step edges shifting the chemical potential to lower values and increasing the probability of metal coordinated molecules at the surface. This situation is reflected by the lower limit of the chemical potential. For constant temperature, the shaded area in Fig. 5 can be interpreted as the partial pressure of available adatoms. The copper coordinated molecular dimerization may be favorable in dependence on the availability of adatoms. The dehydrogenated, metal coordinated dimer is more stable than the hydrogenated one in contrast to the tautomer case where the hydrogenated TA1-M is more stable. Thus, the preferred reaction pathway starts with a metal coordinated TAPP molecule followed by a tautomerization step without loosing the coordination to the adatom. Now, tautomers can dimerize while an additional dehydrogenation is preferred (energy gain compared to TAPP just with dehydrogenation). Like this, more tautomers can be added, resulting in metal coordinated, linear molecular chains. In the end, the preferred reaction pathway depends on the number of adatoms available ranging from an uncoordinated to a metal coordinated polymerization.

4 Summary

Summarizing, we presented detailed first principles investigations of the polymerization process of TAPP molecules on a Cu(111) surface. We have identified the mechanisms that lead to the tautomerization of molecules as a necessary first step (formation of TA1) and the dimer (DI) formation as a second step in the reaction. A catalyzing effect could be attributed to the Cu(111) substrate. It is crucial for the stability of the tautomer TA1, the formation of which is required for the polymerization. We find that metal coordinated (provided the process is accompanied by a dehydrogenation) as well as uncoordinated polymerization processes are possible. The catalytic effect of metallic substrates may thus assist in the formation of covalently bonded molecular networks which are not formed in the gas phase or in solution.

Acknowledgments. Generous grants of computer time from the Höchstleistungsrechenzentrum Stuttgart (HLRS) and the Paderborn Center for Parallel Computing (PC^2) are gratefully acknowledged. We thank the Deutsche Forschungsgemeinschaft for financial support.

References

1. J V Barth, Annu. Rev. Phys. Chem. **58**, 375 (2007).
2. A Nilsson and L G M Pettersson, Surf. Sci. Rep. **55**, 49 (2004).
3. J A A W Elemans, S Lei, and S DeFeyter, Angew. Chem. Int. Ed. **48**, 7298 (2009).
4. S Lukas, G Witte, and C Wöll, Phys. Rev. Lett. **88**, 028301 (2001).
5. Q Chen and N V Richardson, Nature Materials **2**, 324 (2003).
6. S L Tait, A Langner, N Lin, R Chandrasekar, O Fuhr, M Ruben, and K Kern, ChemPhysChem **9**, 2495 (2008).
7. N Nyberg, M Odelius, A Nilsson, and L G M Petterson, J. Chem. Phys. **119**, 12577 (2003).
8. R Pawlak, S Clair, V Oison, M Abel, O Ourdjini, N A A Zwaneveld, D Gigmes, D Bertin, L Nony, and L Porte, ChemPhysChem **10**, 1032 (2009).
9. S Weigelt, C Busse, L Petersen, E Rauls, B Hammer, K V Gothelf, F Besenbacher, and T R Linderoth, Nature Materials **5**, 112 (2006).
10. S F Alvarado, W Rieß, M Jandke, and P Strohriegel, Org. Electronics **2**, 75 (2001).
11. C H Schmitz, J Ikonomov, and M Sokolowski, J. Phys. Chem. C **113**, 11984 (2009).
12. Y Okawa and M Aono, Nature **409**, 683 (2001).
13. O Endo, H Ootsubo, N Toda, M Suhara, H Ozaki, and Y Mazaki, J. Am. Chem. Soc. **126**, 9894 (2004).
14. L Grill, M Dyer, L Lafferentz, M Persson, M V Peters, and S Hecht, Nature Nanotech. **2**, 687 (2007).
15. S Weigelt, C Busse, C Bombis, M M Knudsen, K V Gothelf, T Strunskus, C Wöll, M Dahlbom, B Hammer, E Laegsgaard, F Besenbacher, and T R Linderoth, Angew. Chem. Int. Ed. **46**, 9227 (2007).

16. M Matena, T Riehm, M Stöhr, T A Jung, and L H Gade, Angew. Chem. Int. Ed. **47**, 2414 (2008).
17. M In't Veld, P Iavicoli, S Haq, D B Amabilino, and R Raval, Chem. Commun., 1536 (2008).
18. S Weigelt, C Busse, C Bombis, M M Knudsen, K V Gothelf, E Lægsgaard, F Besenbacher, and T R Linderoth, Angew. Chem. Int. Ed. **47**, 4406 (2008).
19. N A A Zwaneveld, R Pawlak, M Abel, D Catalin, D Gigmes, D Bertin, and L Porte, J. Am. Chem. Soc. **130**, 6678 (2008).
20. M Treier, N V Richardson, and R Fasel, J. Am. Chem. Soc. **130**, 14054 (2008).
21. M Treier, R Fasel, N R Champness, S Argent, and N V Richardson, Phys. Chem. Chem. Phys. **11**, 1209 (2009).
22. J A Lipton-Duffin, O Ivasenko, D. F Perepichka, and F Rosei, Small **5**, 592 (2009).
23. M Matena, M Stöhr, T Riehm, J Björk, S Martens, M S Dyer, M Persson, J Lobo-Checa, K Müller, M Enache, H Wadepohl, J Zegenhagen, T A Jung, and L H Gade, Chem. Eur. J. **16**, 2079 (2010).
24. S Blankenburg, E Rauls, and W G Schmidt, J. Phys. Chem. Lett. **1**, 3266 (2010).
25. J Björk, M Matena, M S Dyer, M Enache, J Lobo-Checa, L H Gade, T A Jung, M Stöhr, and M Persson, Phys. Chem. Chem. Phys. **12**, 8815 (2010).
26. G Kresse and J Furthmüller, Comp. Mat. Sci. **6**, 15 (1996).
27. F London, Z. Phys. Chem. Abt. B **11**, 222 (1930).
28. F Ortmann, F Bechstedt, and W G Schmidt, Phys. Rev. B **73**, 205101 (2006).
29. P E Blöchl, Phys. Rev. B **50**, 17953 (1994).
30. G Kresse and D Joubert, Phys. Rev. B **59**, 1758 (1999).
31. E Rauls, S Blankenburg, and W G Schmidt, Phys. Rev. B **81**, 125401 (2010).